Thermochimica Acta, 138 (1989) 147–160
Elsevier Science Publishers B.V., Amsterdam – Printed in The Netherlands

FACTORS AFFECTING THE THERMAL DECOMPOSITION OF CADMIUM CARBONATE BY TG

LEO REICH, S.H. PATEL and S.S. STIVALA

Department of Chemistry and Chemical Engineering, Stevens Institute of Technology, Hoboken, NJ 07030 (U.S.A.)

(Received 7 March 1988)

ABSTRACT

Various workers have reported contradictory results for the thermal decomposition of cadmium carbonate (CDC) by means of TG (and DTA). Thus, various activation energies E and mechanisms have been reported for this decomposition.

The aim of this paper is to examine various factors which may influence the decomposition of CDC in an attempt to explain the conflicting results previously reported for this decomposition. In this respect, a study of this reaction was made using non-isothermal TG in order to ascertain whether the various factors studied had an appreciable influence on E and mechanism. The various factors employed and discussed were: sample weight, heating rate, type of purge gas, purge gas flow rate and particle size.

INTRODUCTION

Various authors have reported results on the kinetics of the thermal decomposition of cadmium carbonate (CDC) [1–10]. Table 1 lists results obtained for CDC at various ambient conditions. This table indicates the large variations in proposed mechanism and E obtained by different authors.

In view of the above-mentioned contradictory results for the thermal decomposition of CDC, the present authors decided to study CDC decomposition in an attempt to resolve the problem. In this respect, various variables were examined such as heating rate, sample weight, type of purge gas, flow rate of purge gas and particle size, in order to determine their effect on E (kcal mol^{-1}) and the mechanism during the thermal decomposition of CDC using non-isothermal TG (NITG).

EXPERIMENTAL

Material

The CDC was obtained from Aldrich (63.8% Cd and 0.5–2.0 ppm Mg, Al, Fe and Pb). Since the calculated value of Cd for pure CDC should be 65.19%, this product was only about 98% pure with respect to cadmium composition.

TABLE 1

Results reported for the thermal decomposition of CDC

Ambient atmosphere	Mechanism	E(kcal mol^{-1})	Reference
Vacuum	N/A	36	1, 2
CO_2	N/A	39	3
CO_2	N/A	36–160	3
Air	R_3	22	4
Argon	A_3[a]	10	5
Air	A_3[a]	22	6
N/A	R_2	35–39	7
N_2	R_3	36	8
N/A	R_2	N/A	9
CO_2 (6.6 kPa)	F_1	61	10
CO_2 (13.33 kPa)	F_1	70	10
CO_2 (20.0 kPa)	F_1	42	10
CO_2 (26.66 kPa)	F_1	62	10

N/A, not available.

[a] Assumed Avrami mechanism.

Purification of CDC

About 500 ml of distilled water was boiled in a beaker to which about 20 g of CDC was added with vigorous stirring for about 5 min in order to leach out trace impurities. The dispersion thus obtained was allowed to settle down for about half an hour and the upper white turbid layer decanted. The CDC was then filtered through a Whatman no. 1 qualitative filter paper under suction, washed several times with hot distilled water and finally dried in a vacuum oven at 100 °C for at least 2 days. This purified sample was used throughout the present investigation unless it is indicated otherwise.

In order to remove any free $Cd(OH)_2$ from the previously purified CDC, further purification was carried out as follows. About 200 mg sample was placed in a beaker, to which about 100 ml of distilled water was added to make a dispersion of CDC. The beaker was then heated to 80 °C. A calculated amount of 0.1N HCl was added slowly to the dispersion so that 25% of the CDC would be neutralized. It was expected that any free $Cd(OH)_2$ would be neutralized and separated from the CDC. The beaker was kept at 80 °C for half an hour. The CDC was then filtered and dried overnight in a vacuum oven at 90 °C. The results of an elemental analysis on samples treated with boiling water or HCl are given in Table 2 (Schwarzkopf Microanalytical Lab., Woodside, New York).

Particle size determination

The particle size distribution of the purified CDC sample was obtained by using a Cambridge/Olympus Quantimate 10 Image Analyzer. A Zeiss lens

TABLE 2

Elemental analysis of CDC

Element	Boiling water-treated CDC (%)	HCl-treated CDC (%)	Theoretical (%)
Cd	65.24	65.03	65.19
C	6.99	7.32	6.97
H	0.50	0.22	

of magnification 10× was used for the visualization of uniformly spread particles of CDC powder over a glass plate.

The feature distribution of counts by area (μm^2) is shown in Fig. 1. It was found that 97.1% of the total particles were of area < 198 μm^2.

Equipment

A Perkin-Elmer Thermogravimetric Analyzer TGS-2 was used with a System-4 Microprocessor Controller unit and 3600 Data Station. The TG curve data were stored on a mini floppy disk using a TADS software. A printout of weight loss values (%) at any given temperature interval over a given range was obtained using a TADSOFT program developed at Stevens Institute of Technology.

An Apple IIe computer was utilized to estimate kinetic parameters, i.e. activation energy E and mechanism (see Procedure section).

Procedure

A magnetic transition temperature calibration procedure was used for the calibration of TGS-2 using a nickel standard (magnetic transition temperature = 354 ° C).

A typical sample run under given experimental conditions of rate of heating (5, 10, 20 ° C min^{-1}), purge gas flow rate (Ar or N_2 at 20 or 35 cm^3 min^{-1}) and sample weight (~ 5, ~ 12, ~ 20 mg) was made as follows.

The TGS-2 was zeroed at 50 ° C (with purge gas on) and a sample of approximately the required amount was then placed in a platinum sample pan. The sample weight was not entered into the computer memory at this point. The sample was then brought to 250 ° C at a heating rate of 100 ° C min^{-1}, held there for about a minute, the sample weight entered and the experiment started at a given heating rate. After getting a printout of wt.% versus temperature, the degree of conversion α was calculated for a selected number of data pairs, values of which were then utilized for the computation of E and the mechanism using computer methods developed by Reich and

```
Area          Count

               3380          undersize
 198           47            ********************************************************************************
 296           7             ***********
 394           8             *************
 492           3             *****
 590           5             ********
 688           3             *****
 786           0
 884           1             *
 982           2             ***
1080           0
1178           1             *
1276           1             *
1374           1             *
1472           1             *
1570           2             ***
1668           0
1766           0
1864           1             *
1962           2             ***
2060           0
2158           0
2256           0
2354           0
2452           1             *
2550           1             *
2648           0
2746           0
2844           3             *****
2942           2             ***
3040           0
3138           0
3236           0
3334           0
3432           0
3530           0
3628           0
3726           1             *
3824           0
3922           0
4020           0
4118           0
4216           0
4314           0
4412           0
4510           0
4608           0
4706           0
4804           0
4902           0
5000           0
               7             oversize
```

Fig. 1. Histogram showing particle size distribution (by area, μm^2) of CDC.

Stivala, i.e. Method I [11], Method II [12] and Method III [13] (used to corroborate the R_2 mechanism). Method I was modified to account for a broader *E*-range than originally described [14] and this version was utilized in the present investigation. It may be noted here that the purge gas flow rate was calibrated for both Ar and N_2 using a gas-bubble flow meter.

RESULTS AND DISCUSSION

It is well known that the thermal decomposition of CDC is a one-step reaction, $CdCO_3 \rightarrow CdO + CO_2$. The types of mechanisms most frequently

TABLE 3

Kinetic data obtained for the thermal decomposition of CDC in argon using NITG

Run	Heating rate (°C min^{-1})	Sample weight (mg)	Purge gas flow rate (cm^3 min^{-1})	Mechanism	E (kcal mol^{-1})	Computer method
1	5	4.99	20	R_2	32	I
2	5	12.51	20	R_2	31	I
3	5	19.88	20	R_2	31	I
				R_2	31	II
4	10	5.01	20	R_2	30	I
5	10	12.47	20	R_2	29	I
6	10	19.91	20	R_2	28	I
7	20	4.93	20	R_2	30	I
8	20	11.87	20	R_2	31	I
9	20	20.10	20	R_2	28	I
10	5	4.91	35	R_2	32	I
				R_2	32	II
11	5	12.48	35	R_2	31	I
12	5	19.95	35	R_2	32	I
				R_2	32	II
13	10	4.89	35	R_2 [a]	32 [a]	I
		4.97			32	III
14	10	9.97	35	R_2 [a]	30 [a]	I
		9.94			31	III
15	10	19.87				
		19.95	35	R_2 [a]	28 [a]	I
16	20	4.93	35	R_2 [a]	31 [a]	I
		5.02				
17	20	12.30	35	R_2 [a]	29 [a]	I
		12.36				
18	20	19.86	35	R_2	28	I
19	10	5.05	20	R_2 [b]	29 [b]	I
20	10	19.92	20	R_2 [b]	29 [b]	I

[a] Average of duplicate runs.

[b] Finely ground powder.

TABLE 4

Kinetic data obtained for the thermal decomposition of CDC in nitrogen using NITG

Run	Heating rate (°C min^{-1})	Sample weight (mg)	Purge gas flow rate ($\text{cm}^3\ \text{min}^{-1}$)	Mechanism	E (kcal mol^{-1})	Computer method
21	5	5.11	20	R_2 [a]	31 [a]	I
		5.06		R_2 [a]	31 [a]	II
21A	5	5.33	20	R_2	30	I
22	5	12.41	20	R_2	30	I
22A	5	12.42	20	A_3/R_2	11/31	I
				R_2	31	II
23	5	19.99	20	R_3	38	I
				R_3/D_3	37/77	II
23A	5	20.05	20	A_3	11	I
				D_3/R_3	68/33	II
24	10	4.96	20	R_2	31	I
24A	10	4.98	20	R_2 [a]	31 [a]	I
		5.00				
25	10	12.40	20	R_2 [a]	30 [a]	I
		12.43		R_2 [a]	31 [a]	II
26	10	19.96	20	R_3 [a]	32 [a]	I
		19.92		D_3/R_3 [a]	67/32 [a]	II
26A	10	19.94	20	R_3	33	I
				D_3/R_3	68/33	II
27	20	5.04	20	R_2	30	I
28	20	12.43	20	R_2 [a]	30 [a]	I
		12.50		R_2	29 [a]	II
29	20	19.98	20	R_3	30	I
30	5	5.09	35	R_2	28	I
31	5	9.92	35	R_3	34	I
				R_3	35	II
32	5	19.92	35	A_3/R_3	11/34	I
				D_3/R_3	70/34	II
33	10	4.71	35	R_2	30	I
34	10	12.53	35	R_3 [a]	36 [a]	I
		12.53				
35	10	20.55	35	R_3 [a]	34 [a]	I
		20.67				
36	20	5.06	35	R_2	30	I
37	20	12.43	35	R_3	33	I
38	20	20.00	35	R_3	32	
39	5	5.00	20	R_2 [b]	32 [b]	I

[a] Average of duplicate runs.

[b] HCl-treated sample.

mentioned for solid state decomposition reactions are A_4, A_3, A_2, R_2, R_3, F_1, D_1, D_2, D_3 and D_4. Derived kinetic data are shown in Tables 3 and 4, i.e. mechanism and E obtained for the thermal decomposition of CDC in Ar and N_2, respectively, using NITG. The effects of the following variables were examined.

Sample weight (SW) and heating rate (HR)

From Table 3, it can be seen that the variation of sample weight did not have any significant effect on E and the mechanism during the decomposition of CDC in argon, even when the HR or gas flow was varied. Thus, even though the SW was varied from 5–20 mg, the HR from 5–20 °C min^{-1} and the gas flow from 20–35 $\text{cm}^3\ \text{min}^{-1}$, the average value of E was 30.2 ± 1.5 kcal mol^{-1}, and the mechanism obtained was consistently R_2. This can also be seen in Fig. 2.

However, as may be seen from Table 4, the variation of SW had a significant effect on mechanism when CDC was decomposed in the presence

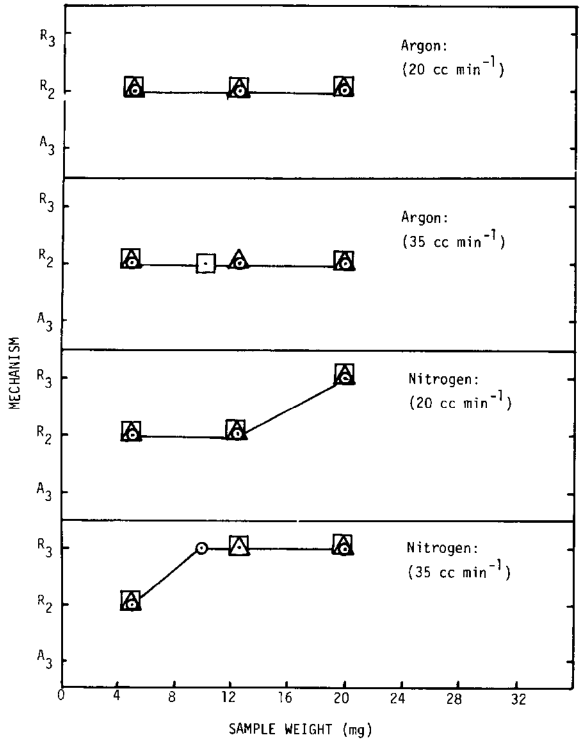

Fig. 2. Dependence of mechanism on SW, HR, type of purge gas and purge as flow rate on the thermal decomposition of CDC. Heating rate: ⊙, 5 °C min^{-1}; □, 10 °C min^{-1}; Δ, 20 °C min^{-1}.

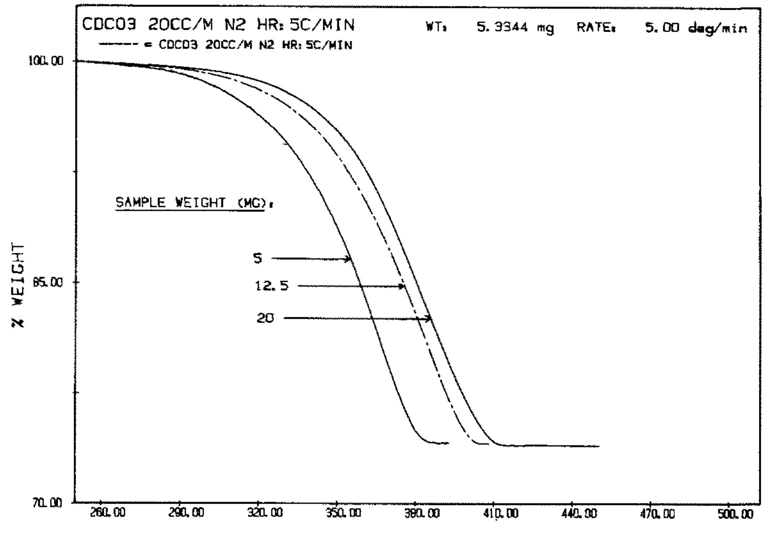

Fig. 3. Typical TG curves showing the effect of SW on the thermal decomposition of CDC.

of nitrogen (also see Fig. 2). For a nitrogen flow rate of 20 cm^3 min^{-1}, the mechanism varied essentially from R_2 to R_3 as the SW varied from 5–20 mg. At a flow rate of 35 cm^3 min^{-1}, the mechanism changed from R_2 to mainly R_3 as the SW varied from 5–20 mg (see also Fig. 2).

Figure 3 clearly indicates the effect of SW on TG curves for the thermal decomposition of CDC in nitrogen. The decomposition temperature in-

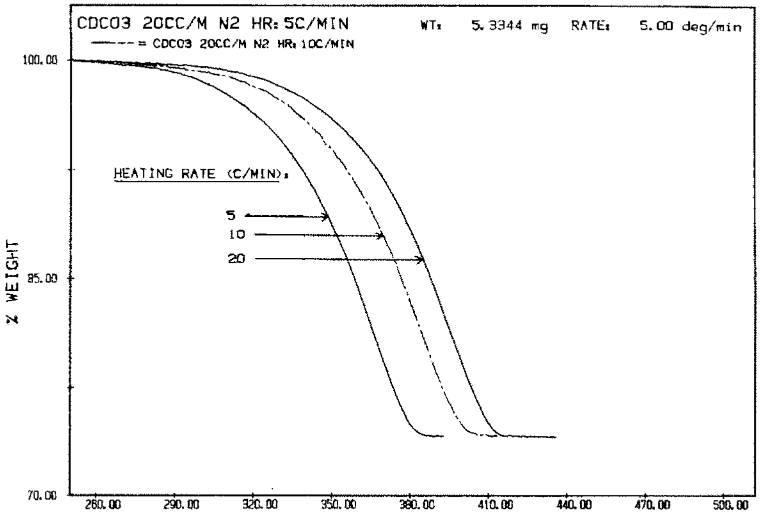

Fig. 4. Typical TG curves showing the effect of HR on the thermal decomposition of CDC.

creases with increase in SW for a given conversion under similar experimental conditions. Tables 3 and 4 show, in general, almost no change in E for argon with increase in SW for the same mechanism. Also, in the case of N_2 (Table 4) for any particular mechanism, the E values did not change much, e.g. for R_2 $E = 30 \pm 0.8$. For the R_3 mechanism $E = 33.5 \pm 1.9$.

The effect of HR on the TG curves is shown in Fig. 4, which indicates the increase in decomposition temperature of CDC with increase in HR for a given conversion as would be anticipated. Recently, Criado et al. [15], during their study on thermal decomposition of $PbCO_3$ under vacuum and under CO_2 pressure, have shown the strong dependence of E and A (Arrhenius pre-exponential factor) on SW. They reported a decrease in E (from 57 to 39 kcal mol^{-1}) with increasing SW (from 1.95 to 4.45 mg) at a given HR (0.5 K min^{-1}) under vacuum assuming a first order kinetic law. Nair and Ninan [16,17] have reported that during the decomposition of CaC_2O_4 to $CaCO_3$, the kinetic parameters, (E and A) obtained from TG data, were not appreciably affected by HR or SW.

Ambient atmosphere

Figure 5 depicts a typical effect of ambient atmosphere on the thermal decomposition of CDC. Thus, when argon was employed, as opposed to nitrogen, the NITG curve shifted to higher temperature, other conditions being similar. Criado and Trillo [18] observed a similar effect: as the

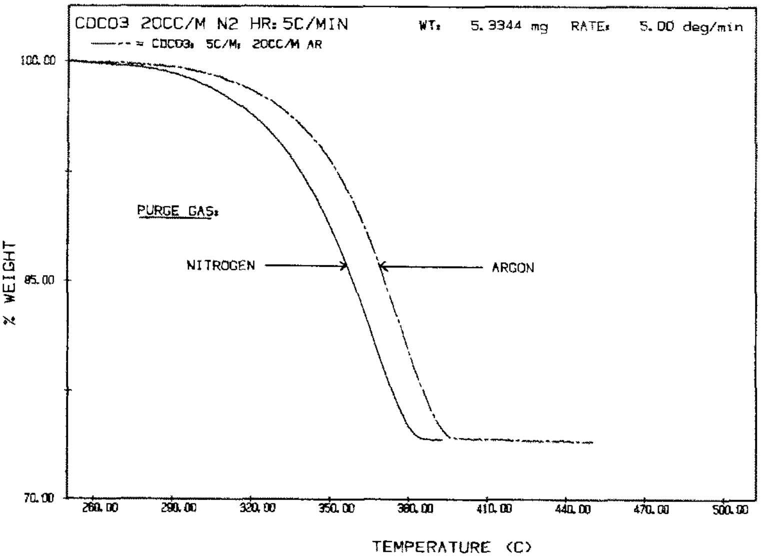

Fig. 5. Typical TG curves showing the effect of type of purge gas on the thermal decomposition of CDC.

molecular weight of the purge gas increased (from He to N_2), the DTA peak during the decomposition of $CaCO_3$ shifted to a higher temperature. It was shown that the shift effect involved solid state reactions which were capable of a reverse equilibrium. Thus, when nickel oxalate (NOX) was subjected to thermal decomposition (an essentially irreversible reaction) by DTA using He and N_2 as purge gases, the DTA peak temperature did not change despite the different experimental conditions used.

Several factors may be involved in the behavior noted above, such as thermal conductivity, molecular weight, adsorption and sample particle size. It is not likely that thermal conductivity is an important factor since the DTA peaks for NOX did not change much whether He or N_2 was utilized as the purge gas. The molecular weight of the purge gas appears to be an important factor. If it is assumed that the diffusivity of a gas increases with decreasing molecular weight, the shift behavior could be readily explained. Thus, since it was previously indicated that this behavior involved only reversible reactions, a purge gas with greater diffusivity would be expected to carry off CO_2 more readily. In this respect, a He–CO_2 mixture would be attained more easily than N_2–CO_2, and N_2–CO_2 more readily than Ar–CO_2.

The adsorption factor should not be overlooked. If the purge gas is adsorbed on the residual CdO surface it could interfere with the reverse equilibrium reaction thereby causing a DTA (or TG) curve to shift to higher temperatures in the case of decompositions involving materials such as $CaCO_3$ or CDC. Indeed, Criado et al. [10] have studied the influence of CO_2 pressure on the kinetics of the thermal decomposition of CDC. They found that as the CO_2 pressure was increased during the decomposition of CDC, the DTG peaks shifted to higher temperatures. The results could be explained if it was considered that CO_2 was chemisorbed on the CdO surface. The active phase boundary would not be the surface covered by CO_2. Utilizing this concept, it was possible to derive an expression from which it could be deduced that the reaction should decrease as CO_2 was increased and, therefore, the resulting DTG curves should shift to higher temperatures, as observed. The expression also predicted that at high CO_2 pressure, an asymptotic value of E would result, in agreement with results obtained. Sample particle size effects will be discussed subsequently.

Purge gas flow rate

The effect of purge gas flow rate (20 or 35 cm^3 min^{-1}) on the TG curves for the thermal decomposition of CDC can be seen in Figs. 2, 6 and 7. No appreciable effect on the decomposition temperature was observed. However, at higher flow rates the decomposition temperature seemed to increase slightly. This could be due to a slightly greater cooling effect at a higher flow rate, thereby necessitating higher decomposition temperatures. Also (Fig. 2), in the case of N_2 purge gas, as the flow rate was increased from 20 to 35 cm^3

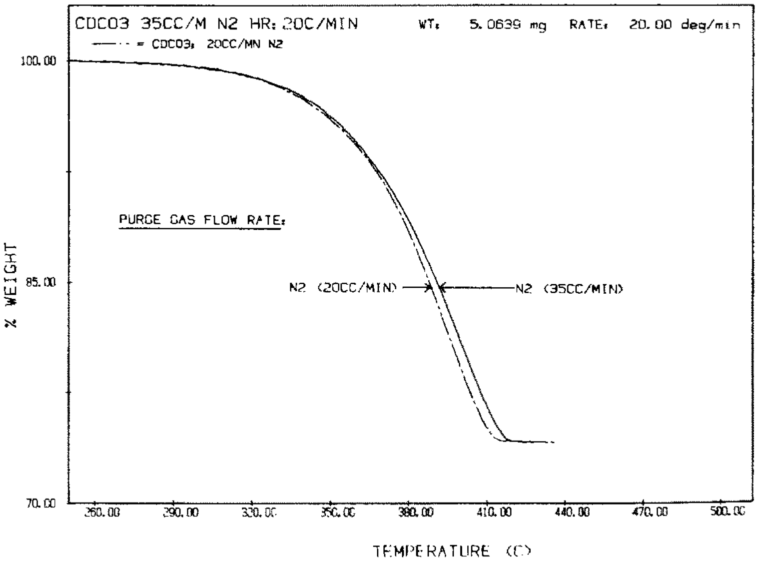

Fig. 6. Typical TG curves showing the effect of purge gas flow rate on the thermal decomposition of CDC.

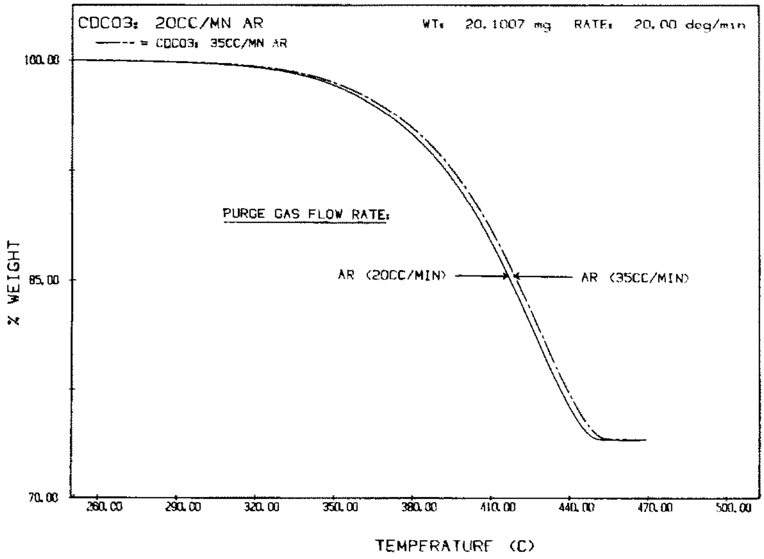

Fig. 7. Typical TG curves showing the effect of purge gas flow rate on the thermal decomposition of CDC.

$\min^{-1}$, the mechanism changed from R_2 to R_3, other conditions being similar (at about 12 mg sample weight).

Particle size

Figure 8 shows the effect of particle size on the TG curves for the decomposition of CDC. A finely ground sample with a smaller particle size than the parent sample indicates a lower decomposition temperature for a given conversion. However, for runs 19 and 20 with the finely ground powder sample, (Table 2), there is not any significant difference in *E* with respect to the parent sample under similar conditions. An HCl-treated sample which also yielded a fine powder, as compared to the parent sample, shows in Fig. 9 a similar trend as in Fig. 8, i.e. a lower decomposition temperature as compared to the parent sample for a given conversion.

Recently, Criado and Gonzalez [19] have studied the effect of grinding on the texture and kinetic stability of CDC and $MnCO_3$, and have indicated that the activation energy decreases with increasing grinding time up to a limit for CDC but remains approximately constant for $MnCO_3$. Criado et al. [20] have reported that grinding of $MgCO_3$, $SrCO_3$ and $BaCO_3$ leads to a decrease in *E*, but in contrast, the enthalpy and *E* of the thermal decomposition of $CaCO_3$ do not undergo significant changes. (This behavior agrees with our observations.)

Miyokawa and Masuda [21] have pointed out the need to take into consideration the effect of particle size distribution while deducing the

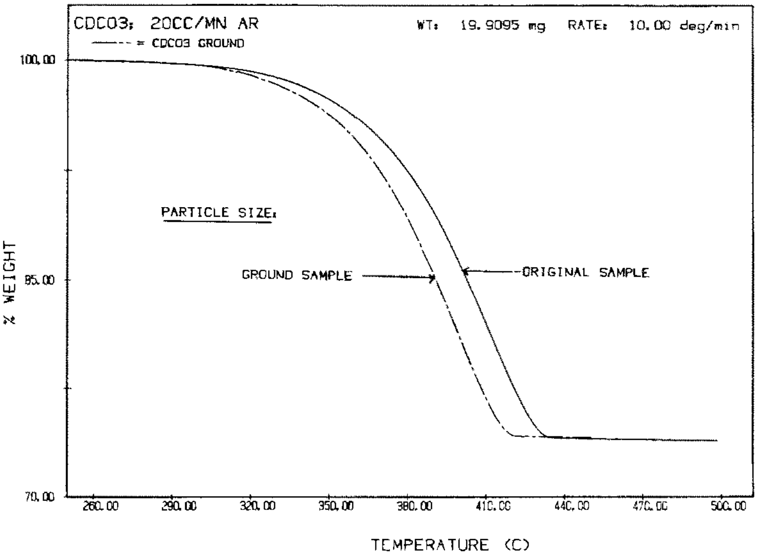

Fig. 8. Typical TG curves showing the effect of particle size on the thermal decomposition of CDC.

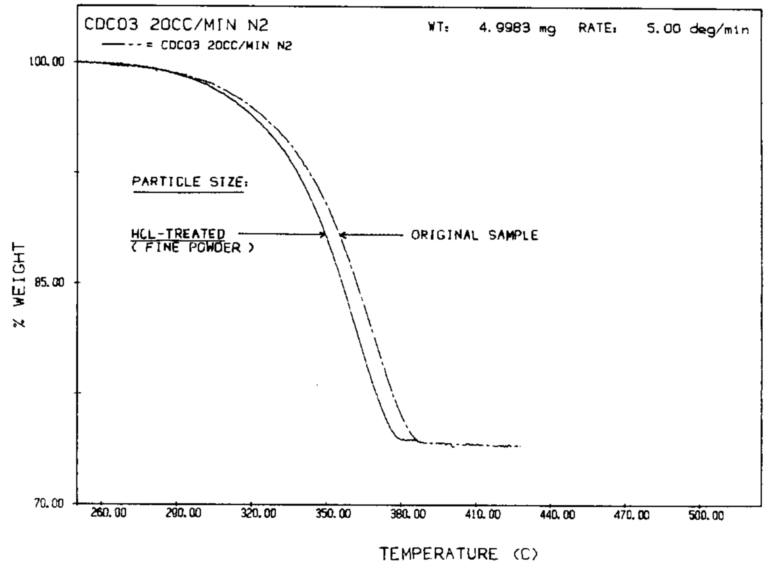

Fig. 9. Typical TG curves showing the effect of particle size on the thermal decomposition of CDC.

kinetic parameters from rate analysis reactions which involved the Avrami equation.

Number of data pairs

It should also be mentioned here that while analyzing the TG data with Methods I or II (or III), the greater the number of data pairs used (15–20) the more reliable the results (in terms of duplicatable values) since more data points represent the TG curve to a greater degree. In the present investigation, Method II has been used as a complement to Method I. Method III was also utilized to spot check contracting geometry mechanisms by yielding corresponding *n* values which were anticipated on the basis of the R mechanism obtained. For example, in run 23A in Table 4, the mechanism determined by Method I was A_3 which appeared to be unusual based on the other results obtained, so Method II was then employed. Method II ruled out A_3 and suggested it to be D_3 or R_3. R_3 was then selected to be the most probable one based on the duplicate run 23. Sharp and Wentworth [22] have also indicated that the number of data pairs could affect the kinetic results. Thus, when the number of points used was increased from 8 to 14, E decreased from 43 to 36 kcal mol^{-1}.

FINAL REMARKS

Our results, as depicted in Fig. 2 and elsewhere, clearly show that for all the experimental variables studied, argon purge gas gives the most consistent results (R_2 mechanism only) whereas N_2 appears to affect the results with respect to HR, SW and purge gas flow rate (R_2 and R_3 mechanisms obtained). This could account for some of the discrepant results depicted in Table 1.

ACKNOWLEDGMENT

The authors would like to express their appreciation and gratitude to Dr. P.K. Bandyopadhyay for assistance with some of the experimental work.

REFERENCES

1 E.A. Prodam and M.M. Pavlyuchenko, Geterogennye Khim. Reaktsii, (1961) 50.
2 E.A. Prodam and M.M. Pavlyuchenko, Geterogennye Khim. Reaktsii, (1961) 79.
3 M.M. Pavlyuchenko and E.A. Prodam, Geterogennye Khim. Reaktsii, (1961) 65.
4 R.S.H. Mikhail, D. Dollimore, A.M. Kamel and N.R. Elnazer, J. Appl. Chem. Biotechnol., 23 (1973) 419.
5 S.R. Dharwadkar, M.S. Chandrasekharaiah and M.D. Karkhanavala, Thermochim. Acta, 25 (1978) 372.
6 S.R. Dharwadkar, A.B. Phadnis, M.S. Chandrasekharaiah and M.D. Karkhanavala, J. Therm. Anal., 16 (1979) 3.
7 A.B. Phadnis and V.V. Deshpande, Thermochim. Acta, 42 (1980) 109.
8 J. Mu and D.D. Perlmutter, Thermochim. Acta, 49 (1981) 207.
9 A.B. Phadnis and V.V. Deshpande, Thermochim. Acta, 62 (1983) 361.
10 J.M. Criado, M. Gonzalez and M. Macias, Thermochim. Acta, 113 (1987) 31.
11 L. Reich and S.S. Stivala, Thermochim. Acta, 73 (1984) 165.
12 L. Reich and S.S. Stivala, Thermochim. Acta, 75 (1984) 405.
13 L. Reich and S.S. Stivala, Thermochim. Acta, 36 (1980) 103.
14 L. Reich and S.S. Stivala, Thermochim. Acta, 76 (1984) 395.
15 J.M. Criado, M. Gonzalez and M. Macias, Thermochim. Acta, 113 (1987) 39.
16 C.G.R. Nair and K.N. Ninan, Thermochim. Acta, 23 (1978) 161.
17 K.N. Ninan and C.G.R. Nair, Thermochim. Acta, 30 (1979) 25.
18 J.M. Criado and J.M. Trillo, J. Thermal Anal., 9 (1976) 3.
19 J.M. Criado and M. Gonzalez, Thermochim. Acta, 79 (1984) 91.
20 J.M. Criado, F. Gonzalez and J. Morales, Thermochim. Acta, 32 (1979) 99.
21 K. Miyokawa and I. Masuda, Thermochim. Acta, 86 (1985) 113.
22 J.H. Sharp and S.A. Wentworth, Anal. Chem., 41 (1969) 14.